A simple modular test rig for measuring static and dynamic friction

Enrico Ciulli[1], Francesca Di Puccio[1] and Lorenza Mattei[1]

[1] Dipartimento di Ingegneria Civile e Industriale, University of Pisa, Pisa, Italy
ciulli@ing.unipi.it, dipuccio@ing.unipi.it, l.mattei@ing.unipi.it

Abstract. In this paper an apparatus for investigations on both static and dynamic friction is described. The apparatus is simple but very modular and can be used in two different configurations: (i) controlling the displacement of an upper specimen connected by an elastic wire to a moving load cell; (ii) controlling the displacement of a lower specimen connected to a moving plate. The capabilities of the apparatus are shown through some preliminary tests that also highlight the several factors that can affect the friction coefficient estimation.

Keywords: Experimental apparatus, friction test, friction force, static and dynamic friction.

1 Introduction

As well known, the coefficient of friction (CoF) is a dimensionless quantity apparently easy to define but often very difficult to be correctly evaluated for specific practical aims, as nicely stressed by Blau in [1]. In fact, friction is a property of the tribological system and is affected by several factors including both surface characteristics (e.g. geometry, materials, texture) and working conditions (e.g. load magnitude and temporal trend, relative motion, lubricating conditions, temperature etc.). Friction can even vary during the service lifetime of the coupling because of damaging processes, such as wear. Consequently, a reliable estimation of the static and kinetic CoFs is a challenging task. To this purpose, after the first solutions proposed by Leonardo da Vinci, reviewed in [2], many different tribometers have been developed. They differ for the measuring concept, the operating conditions and the specimen geometries. As an example, numerous techniques used to measure friction are reported in [3]. The CoF is typically estimated by means of direct/indirect measurements of load/torque using load cells and strain gauges. Among the many factors that can influence friction measurements there is the experimental apparatus itself, as shown for instance in [4], where results obtained under the same working conditions with different tribotesters are presented. In addition, measurement uncertainties due to possible misalignment of specimens and sensors as well as fluctuations of the electrical signals and sensors calibration affect the estimated values of the CoF [5]. Often friction coefficient measurements are conducted according to standards (e.g. ASTM G133 [6], G99 [7] and G115 [8]) that suggest a sufficient number of test repetitions to obtain sufficient data for statistically significant results.

Possible surface modification and formation of wear debris are not easy to be controlled during the test replicas. A novel statistical approach aiming to highlight the most significant time intervals during each test replica is reported in [9]. Because of so different approaches and influences, wide ranges of CoF values can be found in the literature for the same material couplings (variation up to 200%), very often reported without detailing the test conditions. As far as engineering industries are concerned, the risk to select the wrong value of the CoF from published data is significant and should be reduced. The interest for researches on friction has therefore been renewed during the last decade and some new test rigs have been designed to investigate some specific aspects of friction. These new apparatuses, some of which are briefly mentioned below, can take advantage of the continuous improvement of the instrumentation and in some cases also of alternative approaches. As an example, a closed-loop microactuator and a triaxial piezoelectric force transducer are used for measuring the static friction coefficient in [10]. A new approach, based on an electromagnetic digital device, is used in a microtribometer in [11]. An automated apparatus developed to minimize possible human errors in the classical approach based on the inclined plane is employed in [12]. In [13], an automated tribometer is described that provides a single experimental platform able to measure adhesion, wear, kinetic and static friction. A completely different device for measuring static and kinetic CoFs is presented in [14], which is based on the working principle of a mechanical screw to reach very high pressures to simulate metal forming processes. An experimental set-up dedicated to investigations on conditions from macro stick–slip up to stable continuous sliding is used in [15]. In this device, translation displacement and normal load are produced through hydraulic cylinders, while a triaxial piezoelectric force transducer and a piezoelectric accelerometer are used as sensors. The acoustic emission technique is proposed in [16] to identify the onset of relative motion.

The present authors have investigated lubricated [17, 18, 19] as well as dry friction couplings [20] with different specimens and test rigs, i.e. a reciprocating apparatus and a pin-on-disc machine. In order to investigate some of the factors affecting both static and dynamic CoFs, a simple modular experimental apparatus has been developed. Its novel aspect consists in the possibility to be used in two configurations, by actuating one of the two coupled specimens. The apparatus described in this work is addressed to investigated more advanced aspects than in standard tests. Some preliminary results are also described.

2 Experimental apparatus

The experimental test rig was purposely designed for estimating the static and dynamic CoFs from measurements affected by inertial actions in several ways. Other design criteria in the definition of the apparatus were lightness, simplicity, modularity and low-cost.

As shown in Fig. 1, the basement is a legged structure obtained connecting aluminium structural frames by Bosch-Rexroth. Additionally, Aluminium, 7075 (Ergal) and 6082 (Anticorodal), was used for most of the components. On the top of the basement,

two main subgroups can be identified: on the right, there is a plate over which the lower specimen is fixed; on the left there is a 'tower' with the load cell connected to the upper specimen through an elastic wire. The two subgroups can alternatively be fixed or mobile. They can move on two ball rails, with very low friction coefficient (0.002-0.003) and can be connected to the motion transmission system alternatively. In this way, only one actuator is necessary for all types of tests.

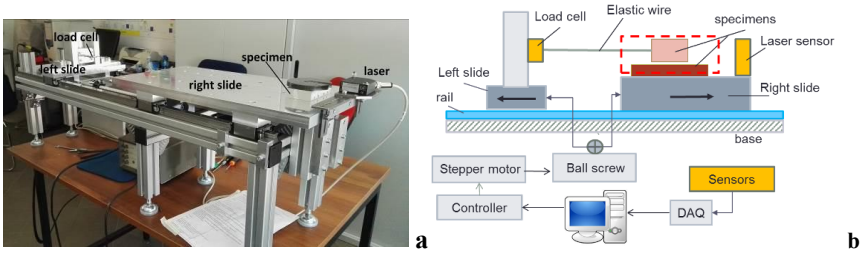

Fig. 1. Photograph (a) and scheme (b) of the apparatus.

A functional scheme of the test rig is represented in Fig. 2. In the case of Fig. 2a, the tower is mobile and the load cell is connected to the upper sliding specimen. The plate with the lower specimen is fixed. In the case of Fig. 2b, alternatively, the plate and the lower specimen are mobile while the upper specimen is constrained by the elastic wire connect to the load cell, that is fixed. The use of the two different configurations allows to investigate in more detail the influence of the inertial actions.

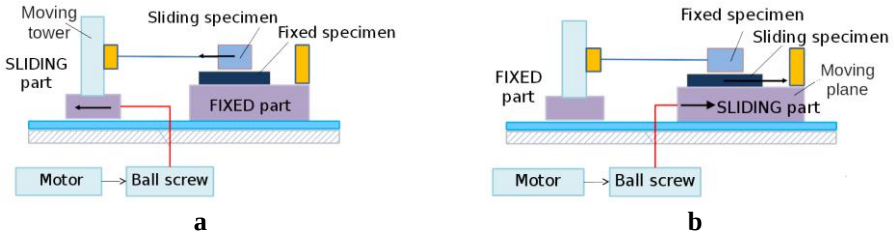

Fig. 2. Functional scheme of the apparatus: (a) upper and (b) lower specimen moving.

The motion transmission system is composed by a ball screw supported by ball bearings connected through an elastic joint to a step motor (1.4 Nm nominal torque and supply voltage 36 V). The angular resolution is 1.8° (200 steps per round) corresponding to a linear resolution of 0.025 mm/step. A micro-step driver can be used that can electronically split the step in 256 parts.

The friction force, horizontal in this apparatus, is measured by a load cell. The load cell is mounted on an adjusting screw that allows the correct alignment of the wire for specimens of different heights (Fig. 3). Two different LSB200 Futek load cells can be alternatively used depending on the maximum friction force to be measured. They have 2 mV/V rated output and 2 N and 100 N full scale. Non linearity and repeatability are

±0.1% and ±0.05% of the rated output respectively. They are temperature compensated between 15 and 72°C.

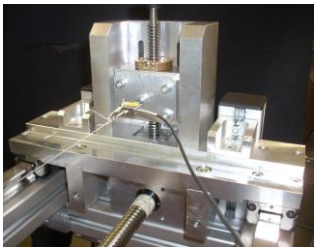

Fig. 3. Detail of the tower with load cell and elastic wire.

Additionally, laser sensors are used to detect the start of the motion and measure the specimen displacement. Two different laser sensors can be alternatively mounted on the test rig: a M5L MEL sensor with a stand-off distance of 24 mm and a measuring range ±0.25 mm, and a LD1302-20 Micro-Epsilon stand-off distance 30 mm and measuring range 20 mm.

An Arduino DUE board is used for managing all electrical and electronic components through a graphical interface specifically developed in Matlab® environment. In this way, user defined motion laws can be easily obtained, with full control of speed and acceleration. Indeed, it was preferred to adopt a displacement controlled loading, being easier and quicker. Thus, in order to obtain a smooth increase of the tangential load transferred to the specimen, an elastic wire is used to pull the specimen. Its stiffness must be properly chosen to control and even avoid oscillations.

A further feature of the apparatus is its possibility to apply a wide range of normal loads (up to 500 N) thanks to the use of dead weights placed over the specimen support. Additionally, the center of gravity of the loaded specimen can be adjusted to be as lower as possible, ideally on the contact surface between the specimens. This is another element that could affect the dynamic of the system.

Specimens can be metallic and non metallic, with conformal or non conformal contacts. In the last case, spheres or cylinders on plane can be used, with the upper elements fixed to suitable support. An example of a plane specimen fixed to the support is shown in Fig. 4. The square specimen is visible in the center of Fig. 4a while it is shown in contact with a plane counter face during a test in Fig. 4b.

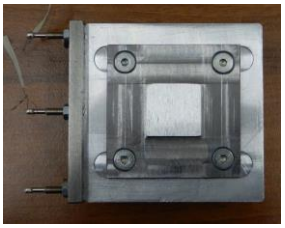

a

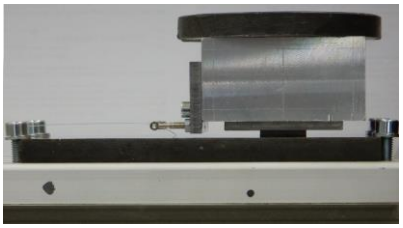

b

Fig. 4. Conformal square specimen mounted to its support (a) and in contact with a plane counter face during a test (b).

3 Test procedure and preliminary results

The first step of the test procedure is the positioning of the specimens after having properly cleaned their surfaces. The upper specimen is connected to the supporting block with screws or glue (Fig. 4a) while the lower specimen is fixed to the plate (Fig. 4b). Then, the upper support is connected to the load cell with a wire. The relative position between the fixed and the moving part (tower or plane) is chosen in order to have the desired length/pre-tensioning of the wire. The supporting block facet must be placed at the stand-off distance of the laser at the beginning of the test. Using the software interface, the desired law of the speed is established assigning time-velocity data pairs, as well as the number of data points to be recorded during the test. As output data, the force measured by the load cell and the displacement measured by the laser are recorded in a file with the correspondent sample time. The movement of the block can also be recorded by a camera. A high speed camera can also be used for detection of high frequency motions, a PCO 1200-HS with an internal memory of 4GB and a resolution of 1280x1025 pixels. The camera is able to take pictures with a frame rate up to 1000 fps that can be increased by reducing the image dimension up to 30000 fps with the minimum 16 pixels window.

Some experimental tests were carried out in order to check the functionality of the apparatus. Tests were performed with a conformal contact using the specimen shown in Fig. 4.

A simple trapezoidal law was used for the speed with a linear trend from zero to the desired maximum speed in 1 s and similarly for the deceleration. The duration of a complete test was 10 s. Three values of the maximum speed were imposed: 0.5-1-2 mm/s to investigate the speed influence on the CoF. It must be observed that, due to some clearances and to the compliance of the wire, the effective actuation on the specimen could slightly differ from the profile described above.

Tests were carried out with two normal loads, 6 and 11.6 N, producing a mean contact pressure of 15 kPa and 29 kPa, respectively. They were combined with the three maximum speeds and also with different actuated part (tower/plate).

Only some sample results of tests carried out at 0.5 and 1 mm/s are reported in the following due to lack of space.

The effect of the maximum speed of the actuator is shown in Fig. 5 for the case of mobile tower. Data were collected at the sampling rate of 1000 samples/s. Classical stick-slip effects are evident. It can be observed that, as the speed increases, also the number of peaks increases. As expected, doubling the speed produces approximately a double number of the force peaks (remember that during the first and the last seconds the speed is not constant). Additionally, the maximum and minimum force values of each fluctuation differ more by increasing the speed. Note that the wire is pre-tensioned at the beginning of the tests. Differences among the two plots depend on the speed but also on other elements as already observed: local surface conditions, pre-tension and also vibrations.

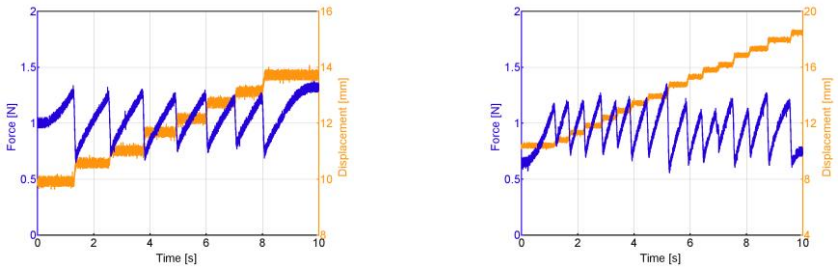

Fig. 5. Measured force and displacement vs. time on a conformal contact. Comparison of 2 maximum speeds: 0.5 mm/s (a), 1 mm/s (b). Moving tower; load: 6 N.

Fig. 6 shows the results obtained for the same speed used in tests of Fig. 5 with an almost doubled normal load (11.6 N). As expected, a duplication of the normal load corresponds roughly to a duplication of the measured force. It is to be noted that signals are more stable, in particular the one of the force (reduced influence of vibrations). As far as the speed influence is concerned, observations similar to the ones for the normal load of 6 N can be confirmed.

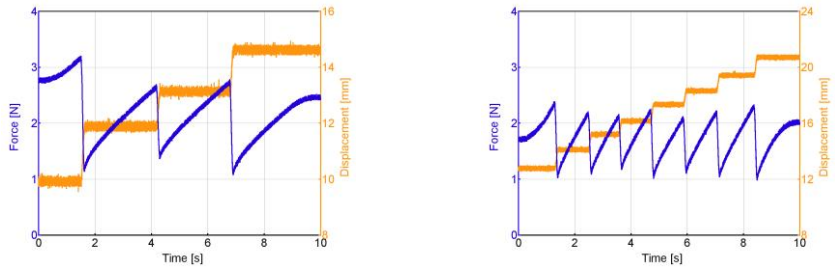

Fig. 6. Measured force and displacement vs. time on a conformal contact. Comparison of 2 maximum speeds: 0.5 mm/s (a), 1 mm/s (b). Moving tower; load: 11.6 N.

The tests concerning the plots shown in Fig. 5 were repeated changing the actuation, i.e. moving the plane rather than the tower. The recorded force and displacement trends are shown in Fig. 7. The measured force is greater than in the case of moving tower, which produces less peaks. This could be related to less vibrations, as vibrations are usually related to a decrease of friction, but also to some inertial effects that will be investigated in the future. It was found that these differences decrease by increasing the normal load, which should reduce the influence of the vibrations.

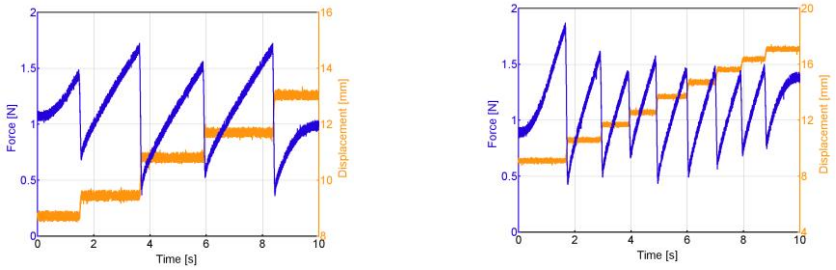

Fig. 7. Measured force and displacement vs. time on a conformal contact. Comparison of 2 maximum speeds: 0.5 mm/s (a), 1 mm/s (b). Moving plane; load: 6 N.

4 Concluding remarks and future developments

A novel apparatus for investigations on static and dynamic friction is described, which has some elements of originality with respect to the solutions available on the market or described in the literature.

Some preliminary experiments have highlighted the capabilities of the experimental apparatus and a few of the many factors that affect the estimation of the coefficient of friction. In particular, the sliding speed and the normal contact were considered. As results, plots of the measured force and displacement vs. time are reported and briefly discussed.

As a peculiarity of the apparatus, some tests were performed with the actuation alternately applied to the one of the two specimens, showing the effect of the inertial actions on the CoF measurements.

The preliminary results have raised some interesting issues that will deserve further investigations as the influence of the dwell time before starting the test, the influence of vibrations, the effect of a deep cleaning of the surface. Additionally, the difference of friction in conformal and non-conformal contacts will be investigated.

Despite friction evaluation appears as a rather simple experimental question, the discrepancies between results from tests performed in apparently very similar conditions highlight how hard it is to provide a reliable value for practical applications.

Acknowledgments The authors would like to thank Mr. Marco Mancino for his contribution to the experimental activity and Ing. André Boiocchi of Luchsinger srl for providing the LD1302-20 Micro-Epsilon laser sensor.

5 References

1. Blau, P.J.: The significance and use of the friction coefficient. Tribology International, 34(9), 585-591 (2001) https://doi.org/10.1016/S0301-679X(01)00050-0
2. Hutchings, I.M.: Leonardo da Vinci's studies of friction. Wear, 360-361, 51–66 (2016) https://doi.org/10.1016/j.wear.2016.04.019

3. Budinski, K.G.: Laboratory Testing Methods for Solid Friction. In: Blau P.J., editor. ASM Handbook, Volume 18: Friction, Lubrication, and Wear Technology. Materials Park Ohio, ASM International, pp. 45-58 (1992)
4. Trzos, M. and Cortés, D.M.: The effect of the test condition on the scatter of the friction coefficient measurements. Scientific Problems in Machines Operations and Maintenance, 2(162), 7-18 (2010)
5. Schmitz, T.L., *et al.*: The difficulty of measuring low friction: Uncertainty analysis for friction coefficient measurements. ASME Journal of Tribology, 127(3), 673-678 (2005)
6. ASTM G133-05(2016). Standard Test Method for Linearly Reciprocating Ball-on-Flat Sliding Wear.
7. ASTM G99-17. Standard Test Method for Wear Testing with a Pin-on-Disk Apparatus
8. ASTM G115-10(2018). Standard Guide for Measuring and Reporting Friction Coefficients.
9. Liguori, C. *et al.*: A Statistical Approach for Improving the Accuracy of Dry Friction Coefficient Measurement. IEEE Transactions on Instrumentation and Measurement 68(5), 8684274, 1412-1423 (2019) https://doi.org/10.1109/i2mtc.2018.8409747.
10. Lee, C-H. and Polycarpou, A.A.: Static friction experiments and verification of an improved elasti-plastic model including roughness effects. ASME Journal of Tribology, 129(4), 754-760 (2007)
11. Petit, L., *et al.*: Presentation of a new method to measure the friction coefficient using an electromagnetic digital device. Proc Inst Mech Eng Part J J Engineering Tribology, 224(9), 1019-1026 (2010)
12. Ibrahim Dickey, R.D., *et al.*: Measurements of the static friction coefficient between tin surfaces and comparison to a theoretical model. ASME Journal of Tribology, 133(3), 1-7 (2011)
13. Kalihari, V., *et al.*: An automated high throughput tribometer for adhesion, wear, and friction measurements. Review of Scientific Instruments, 84(3), 1-9 (2013)
14. Pougis, A., *et al.*: Dry friction of steel under high pressure in quasi-static conditions. Tribology International, 67, 27-35 (2013)
15. Tonazzi, D., *et al.*: Experimental and numerical analysis of frictional contact scenarios: from macro stick–slip to continuous sliding. Meccanica, 50(3), 649-664 (2015) https://doi.org/10.1007/s11012-014-0010-2
16. Taura, H. and Nakayama, K. Behavior of acoustic emissions at the onset of sliding friction. Tribology International, 123, 155-160 (2018) https://doi.org/10.1016/j.triboint.2018.01.025
17. Bassani, R. and Ciulli, E. Friction in boundary and mixed lubricated line contacts with different roughness. In: Thinning Films and Tribological Interfaces, Trib Ser 38, pp. 759-768 (2000)
18. Ciulli, E., *et al.*: The influence of the slide-to-roll ratio on the friction coefficient and film thickness of EHD point contacts under steady state and transient conditions. Tribology International, 42(4), 526-534 (2009) https://doi.org/10.1016/j.triboint.2008.04.005
19. Di Puccio, F. and Ciulli, E. Theoretical and experimental investigation on friction in lubricated line contacts with different materials and textures in presence of wear. Key Eng Mat, 681,142-154 (2016) https://doi.org/10.4028/www.scientific.net/KEM.681.142
20. Ciulli, E. *et al.*: Friction and wear comparison tests on different surface coatings and shapes. In: Proceedings of IFToMM World Congress 2015, Taipei, pp. 1-8 (2015) https://doi.org/10.6567/IFToMM.14TH.WC.OS18.022